Supplement of Earth Syst. Dynam., 11, 415–434, 2020
https://doi.org/10.5194/esd-11-415-2020-supplement

Earth System Dynamics
Open Access
EGU

Supplement of

Differing precipitation response between solar radiation management and carbon dioxide removal due to fast and slow components

Anton Laakso et al.

Correspondence to: Anton Laakso (anton.laakso@fmi.fi)

Supplement

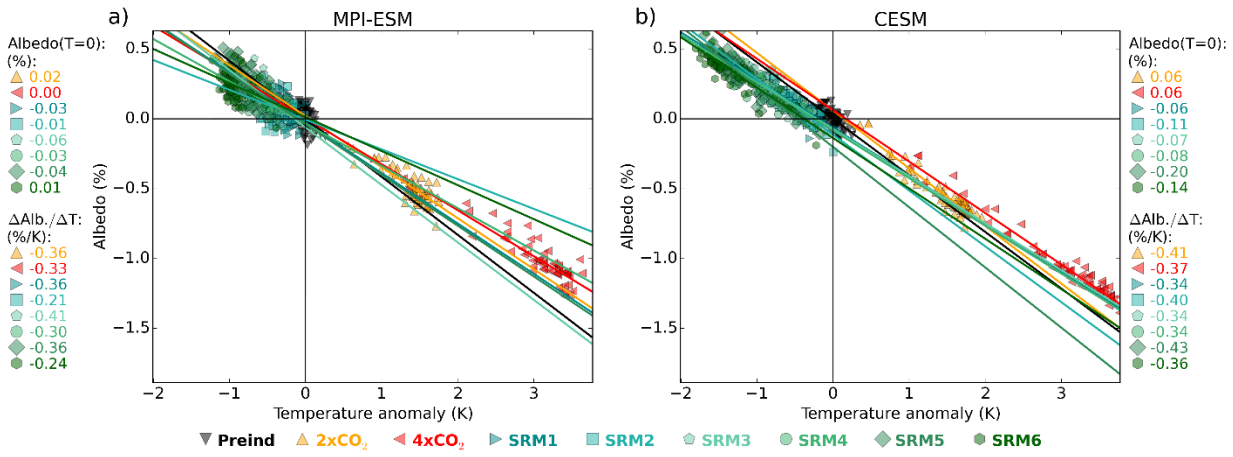

Figure S1: Gregory plots of albedo change for a) MPI-ESM and b) CESM. Markers indicate a single-year global mean value for one ensemble member and solid lines are linear fits. Origin represents zero temperature and albedo anomaly compared to the Preind simulation.

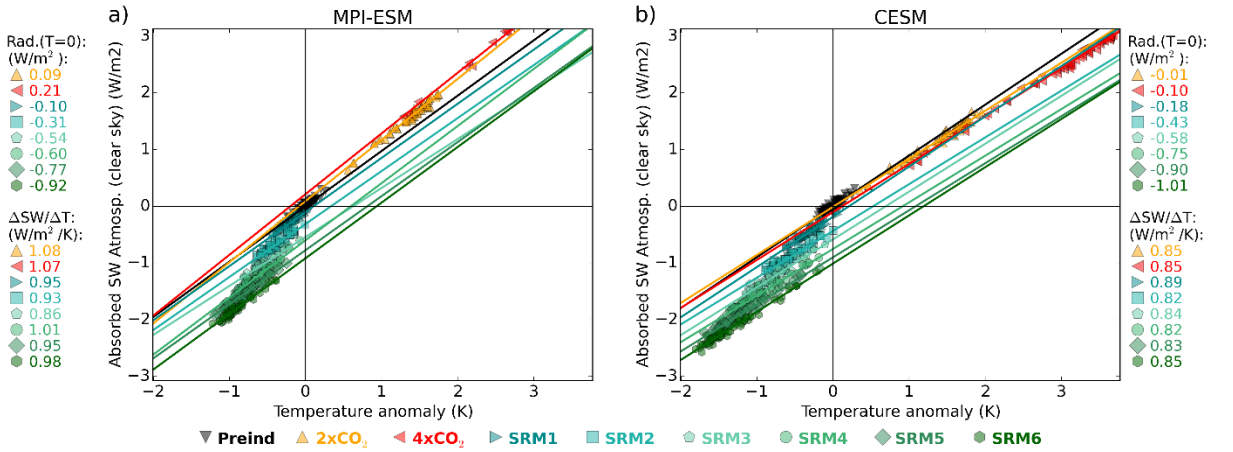

Figure S2: Gregory plots of clear sky atmospheric absorption change for a) MPI-ESM and b) CESM. Markers indicate a single-year global mean value for one ensemble member and solid lines are linear fits. Origin represents zero temperature and atmospheric absorption anomaly compared to the Preind simulation.

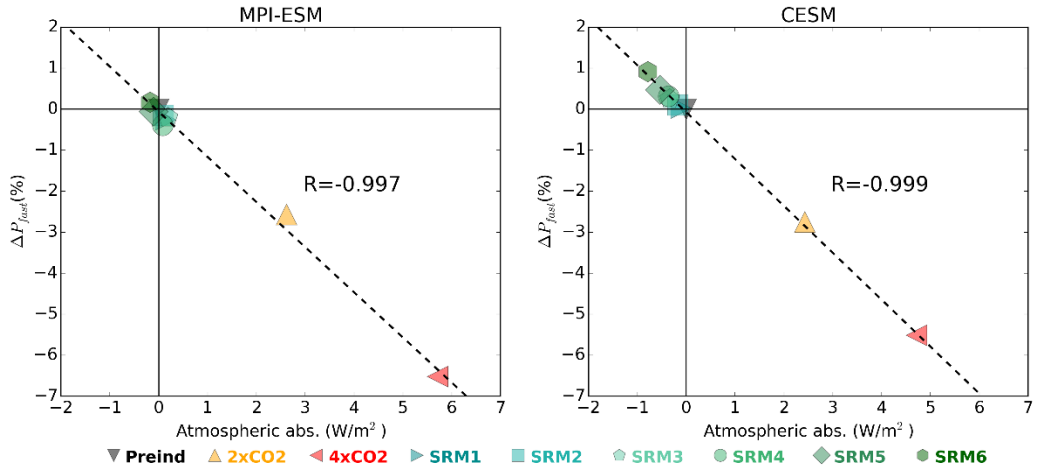

Figure S3. Regression of fast precipitation response versus atmospheric absorption in a) MPI-ESM and b) CESM. R is the Pearson correlation coefficient.

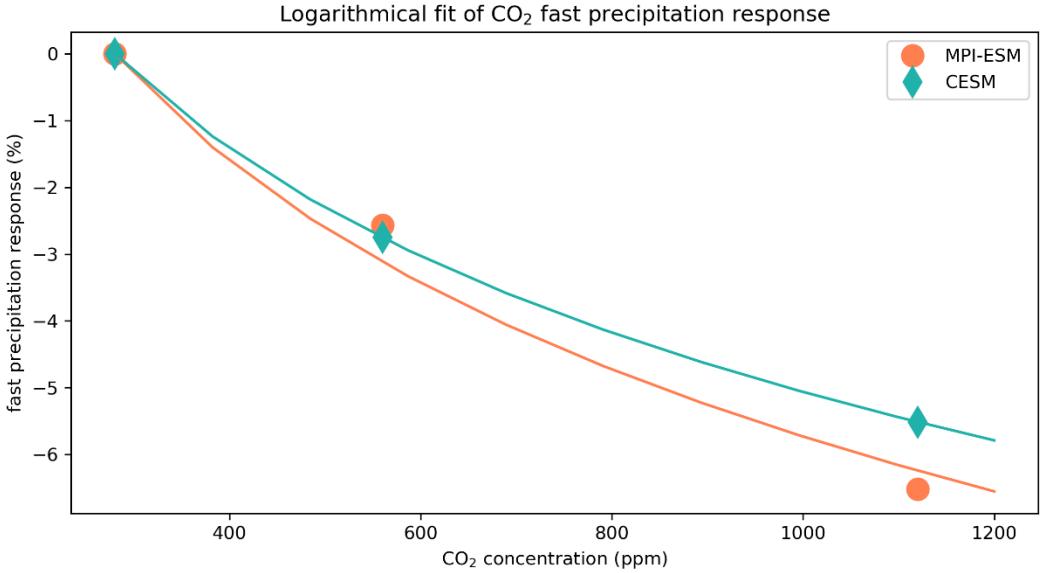

Figure S4. Logarithmical fit of CO2 fast precipitation calculated from preind, 2xCO2 and 4xCO2 scenarios.

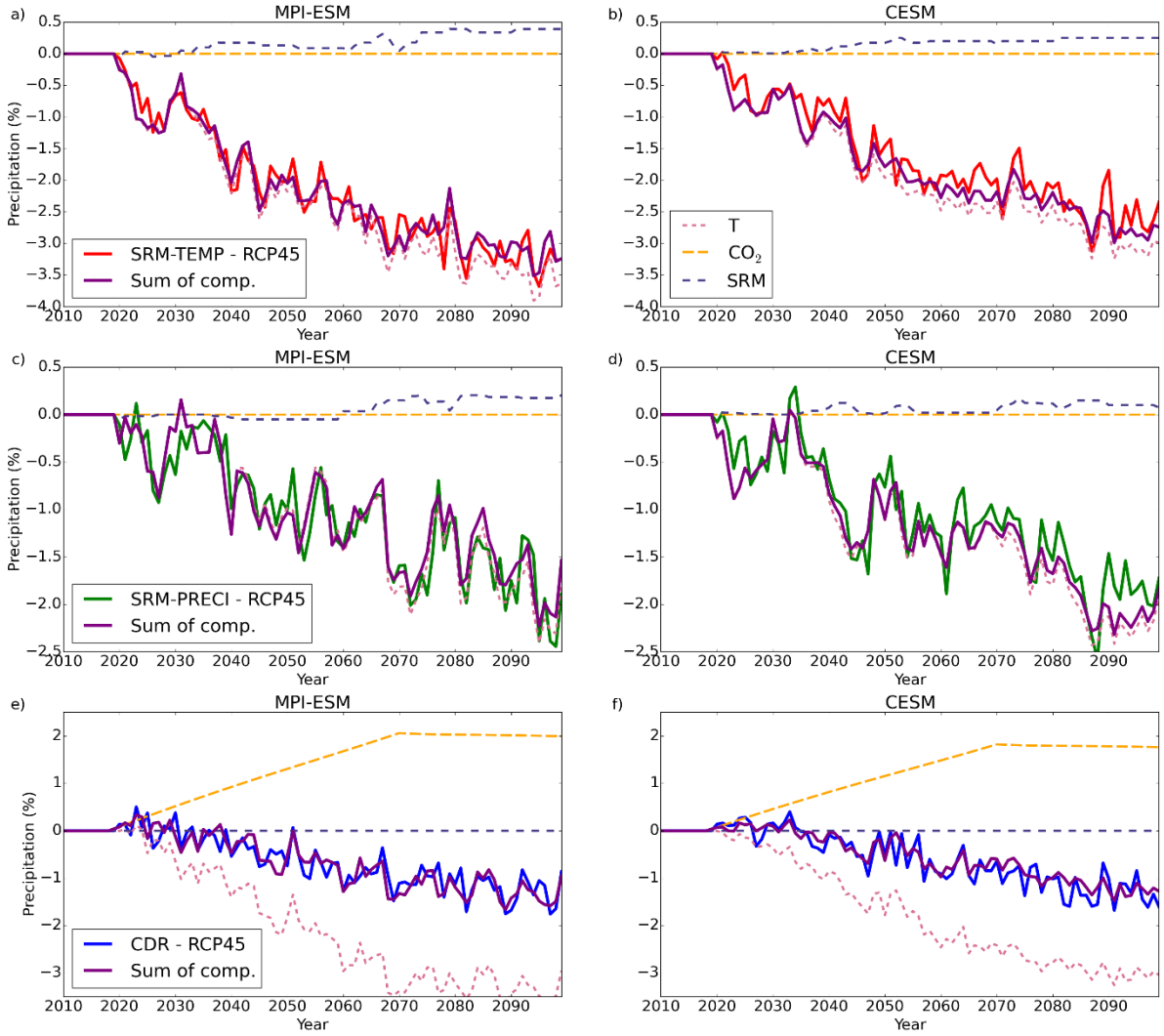

Figure S5. Precipitation and precipitation components for each geoengineering scenario compared to RCP45.

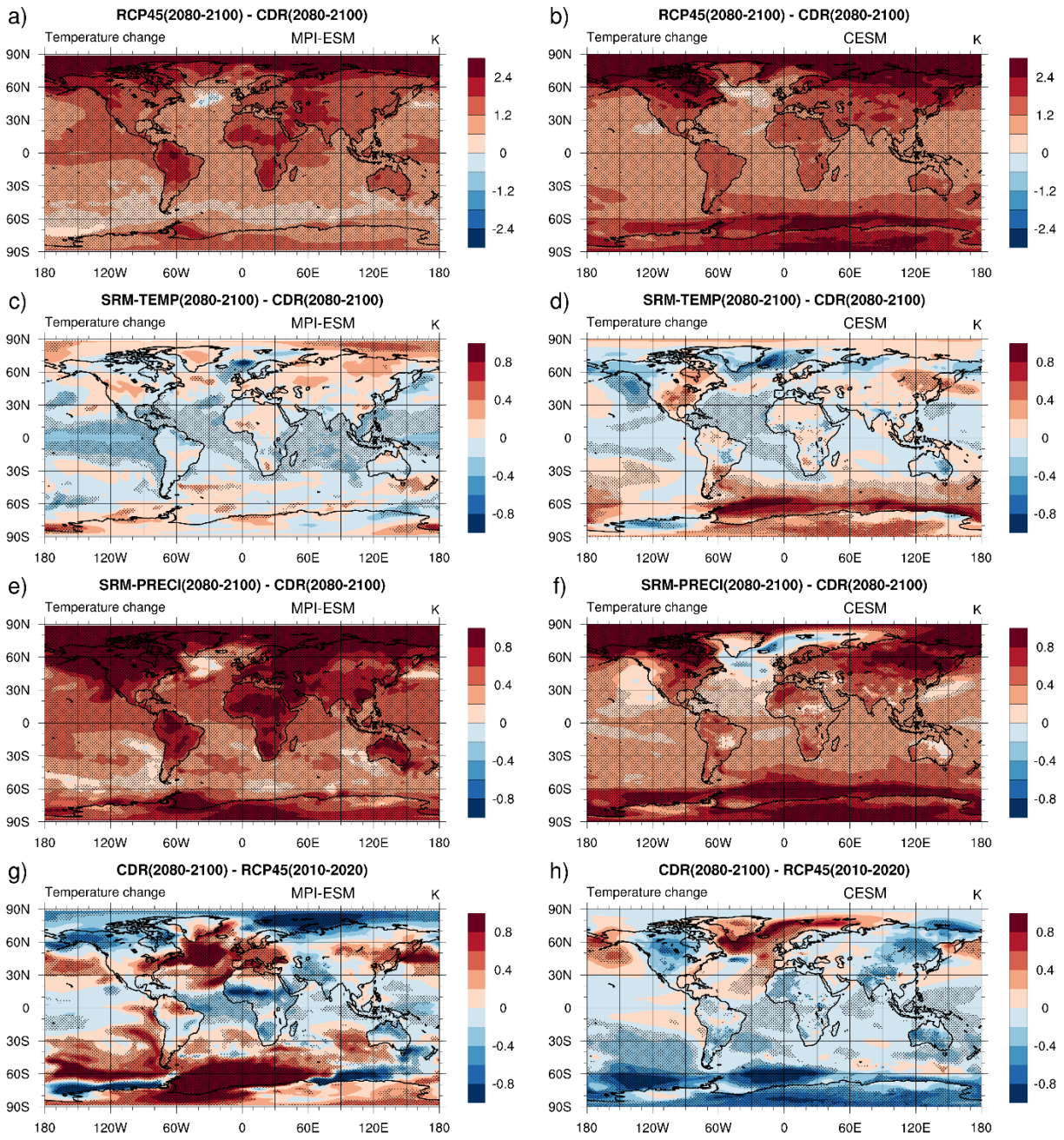

Figure S6. Regional temperature differences between a-b) RCP45 and CDR, c-d) SRM-TEMP and CDR, and e-f) SRM-PRECI and CDR for years 2080-2100. Also shown are the temperature differences between g-h) CDR in years 2080-2100 and RCP45 in years 2010-2020. The left and right columns show results for MPI-ESM and CESM, respectively. Stippling indicates regions where the temperature change is statistically significant at the 95% level, with significance levels estimated using a Student's paired *t*-test (sample of 20 yearly mean values for 3 ensemble members).

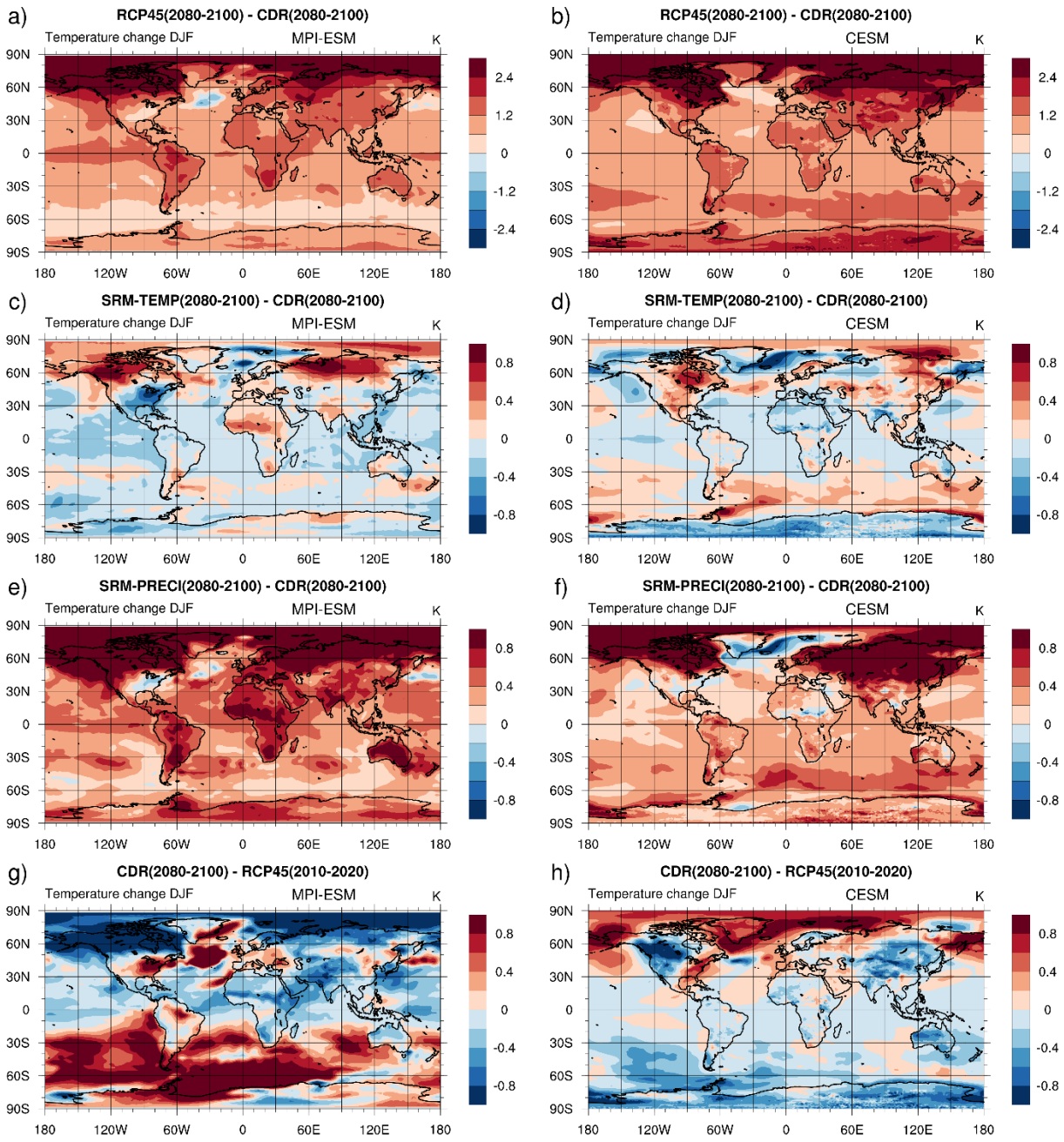

Figure S7. Regional temperature differences in December-January-February between a-b) RCP45 and CDR, c-d) SRM-TEMP and CDR, e-f) SRM-PRECI and CDR in years 2080-2100. Also shown are the temperature differences between g-h) CDR in years 2080-2100 and RCP45 in years 2010-2020. The left and right columns show results for MPI-ESM and CESM, respectively.

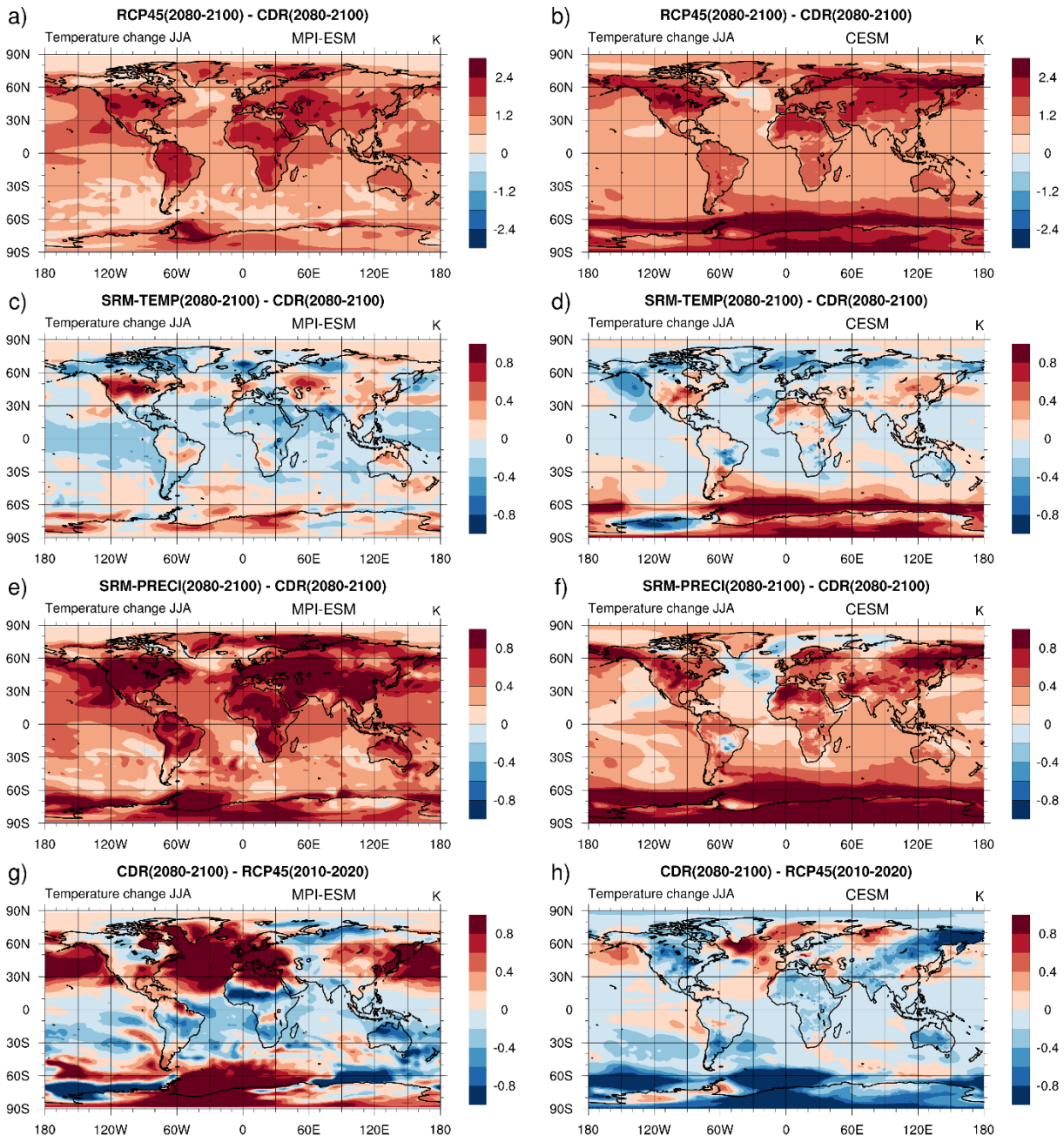

Figure S8. Regional temperature differences in June-July-August between a-b) RCP45 and CDR, c-d) SRM-TEMP and CDR, e-f) SRM-PRECI and CDR in years 2080-2100. Also shown are the temperature differences between g-h) CDR in years 2080-2100 and RCP45 in years 2010-2020. The left and right columns show results for MPI-ESM and CESM, respectively.

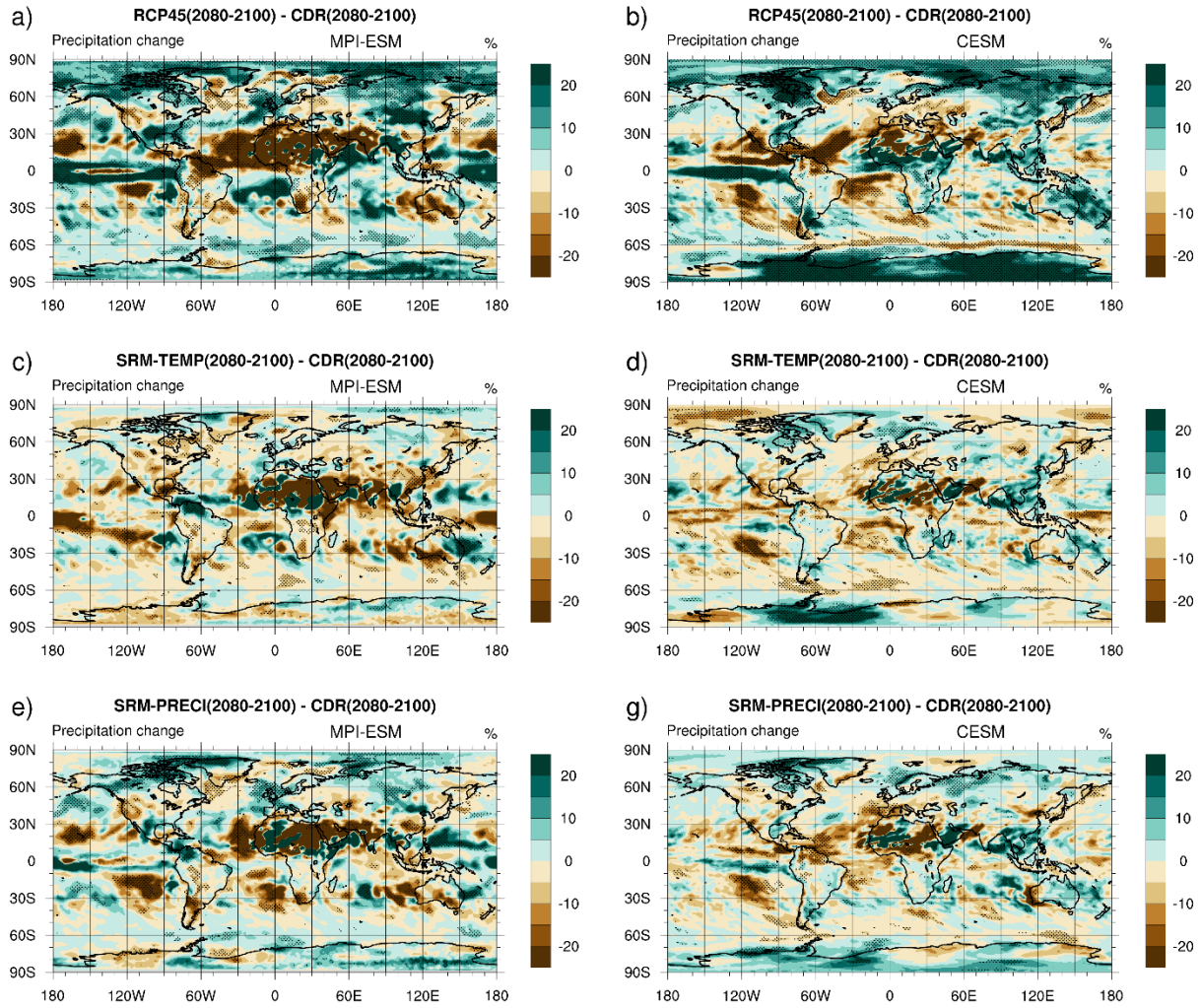

Figure S9. Regional precipitation differences in December-January-February between a-b) RCP45 and CDR, c-d) SRM-TEMP and CDR and e-f) SRM-PRECI and CDR in years 2080-2100. Stippling indicates regions where the temperature change is statistically significant at the 95% level, with significance levels estimated using a Student's paired *t*-test (sample of 20 yearly mean values for 3 ensemble members).

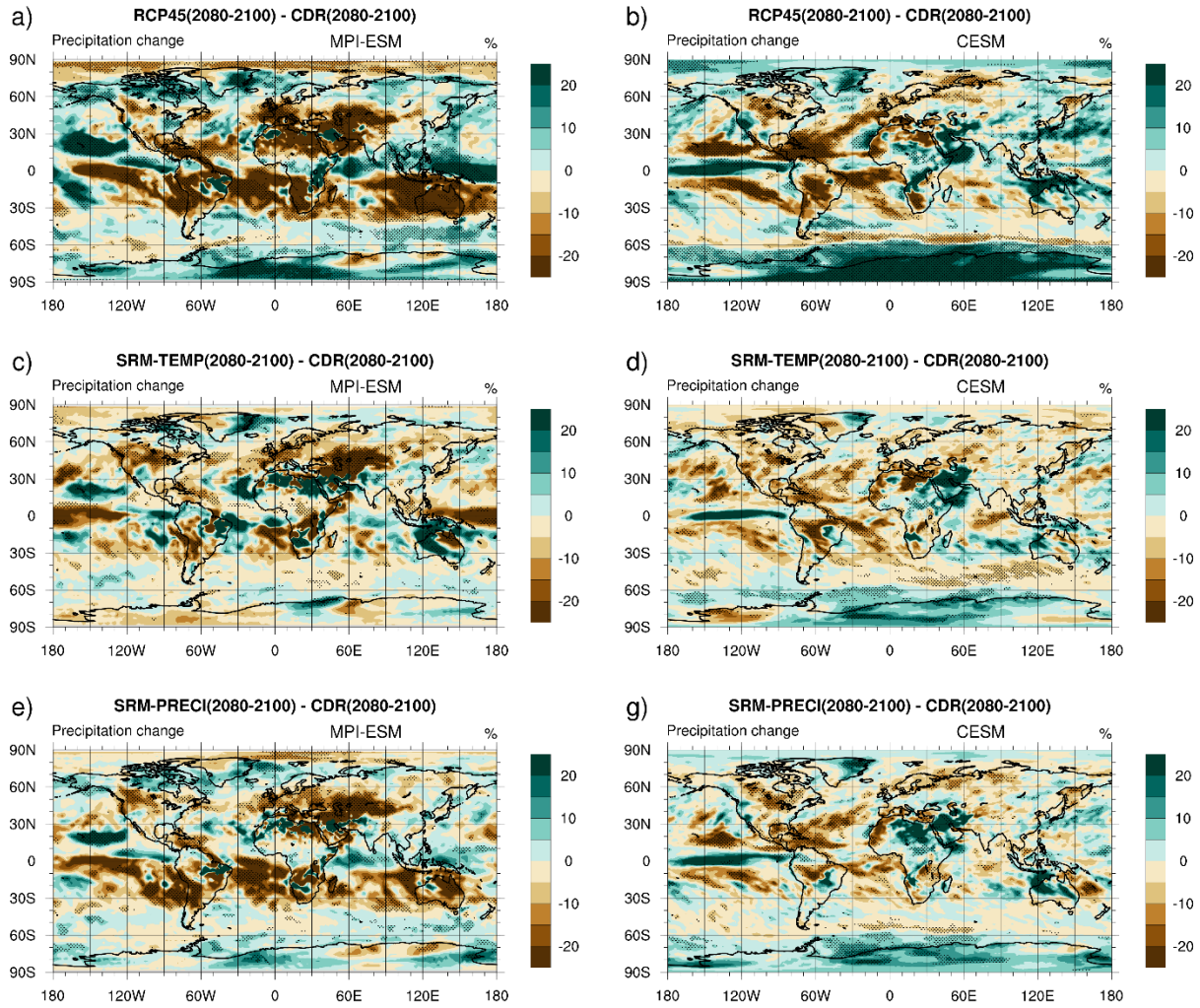

Figure S10. Regional precipitation differences in June-July-August between a-b) RCP45 and CDR, c-d) SRM-TEMP and CDR and e-f) SRM-PRECI and CDR in years 2080-2100. Stippling indicates regions where the temperature change is statistically significant at the 95% level, with significance levels estimated using a Student's paired *t*-test (sample of 20 yearly mean values for 3 ensemble members).